Astronomy & Astrophysics manuscript no. StellarInteriors
February 8, 2020

Polytropic Stellar Models: On the study of stellar interiors

Project II - Computational Astronomy

Ana C. Barboza

[1]

December 2019

ABSTRACT

Aims. We aim to develop an algorithm that implements the fundamental equations and boundary conditions that describe the physics of stellar interiors, allowing us to reach conclusions regarding their structure.
Methods. The Lane-Emdem equation is solved so as to gather ρ, P, and T at each distance r from the center of the star. This information is then used to calculate the emissivity ϵ and luminosity, assuming that the main source of energy is the fusion of Hydrogen (main sequence stars). We then look at the aforementioned quantities and draw conclusions. Three stars are studied in order to implement our method: Gliese 892, Gamma Pavonis and Procyon A.
Results. A method for the study of stellar interiors is provided, and conclusions regarding its limitations discussed.

Key words. stellar interiors – polytropes

1. Introduction

One of the main goals of astronomy and astrophysics is the study of stars. This means not only gathering direct information regarding their radius, mass and luminosity (for example, through the study of binary systems), but also developing methods to use this data, together with physical models, in order to obtain a fuller description of these objects.

In this work, our goal is to study stellar interiors. As in every physical system, the first step is to simplify the problem, namely assuming spherical symmetry and the absence of electromagnetic forces, followed by establishing the equations and boundary conditions that define the problem. After setting these, they translate to two structure equations dealing with three different quantities: m, ρ and P. Polytropic models come as as a way of relating these thermodynamic quantities, compacting the problem into one single expression - *the Lane-Emden equation*, and reducing it to the determination of the best polytropic index n that fits given input.

2. Physics of the problem

Bearing in mind the conservation of mass, the hydrostatic equilibrium, as well as the Poisson equation for a grativational potential, one can find the relations (1) and (2), as in Monteiro (2019):

$$\frac{\mathrm{d}P}{\mathrm{d}r} = -\frac{Gm\rho}{r^2} \tag{1}$$

$$\frac{\mathrm{d}m}{\mathrm{d}r} = 4\pi r^2 \rho \tag{2}$$

We can use a polytropic model for stars to relate above equations, which is given by equation (3).

$$P = K\rho^{1+\frac{1}{n}} \tag{3}$$

After some algebraic manipulation and defining new quantities (ξ, θ) given by $\theta^n \equiv \rho/\rho_c$ and $\xi \equiv r/a$, the whole problem can now be rewritten as in (4), the well known Lane-Emden equation,

$$\frac{1}{\xi^2}\frac{d}{d\xi}\left(\xi^2 \frac{d\theta}{d\xi}\right) = -\theta^n \tag{4}$$

For which solutions can be found if inicial/boundary conditions are set, and will depend on n.

2.1. Boundary conditions

The first initial condition at $\xi = 0$ follows directly from the definition of θ,

$$\rho(r = 0) = \rho_c \Rightarrow \theta(\xi = 0) = 1 \tag{5}$$

For $d\theta$, we define it as:

$$\left.\frac{\mathrm{d}\theta}{\mathrm{d}\xi}\right|_{\varepsilon=0} = 0 \tag{6}$$

2.2. Determination of the polytropic index

A full description of the polytrope and the determination of its solutions requires a determination of n and K. For the case of main sequence stars this is very straightforward, since the main source of energy is the fusion of Hydrogen in their cores. The emissivity ε will be due to the energy production corresponding to the two reactions that make up this process, PP chains (equation 7) and the CNO cycle (equation 8), (Monteiro (2019)), (Monteiro et al. (2019)).

$$\varepsilon_{\mathrm{pp}} \simeq \varepsilon_{\mathrm{pp},0} X^2 \rho T^4 \tag{7}$$

$$\varepsilon_{\rm cno} \simeq \varepsilon_{\rm cno,0} X X_{\rm cno} \rho T^{16} \tag{8}$$

We can then integrate ε and obtain the luminosity.

$$\frac{L_r}{L} = \frac{1}{\xi_s^2 (-\theta'_s)} \int_0^{\xi} \xi^2 \theta^n \left(\frac{M}{L}\varepsilon\right) \mathrm{d}\xi \tag{9}$$

The polytropic index n is determined such that, calculating L through (9), it equals the observed value ($L_r(R) = L_*$). This is done by calculating the zero of $y(n)$:

$$y(n) \equiv 1 - \frac{L_r(R)}{L} \tag{10}$$

After obtaining this value, we simply plug it into (4) and get the behavior of the thermodynamic quantities that describe the star's interior. There's no need for explicitly calculating K, since the equations that describe these will not depend on this value, as mentioned below.

2.3. Structure determination

For each solution curve, whose behavior is shown in figure (1), we get a set of values ξ, θ, θ' that allow us to determine how the pressure P, temperature T and density ρ vary with ξ. We can also get an expression for $M(r)/M_*$. These relations are given by (11) to (14), as in Monteiro (2019):

$$\rho = \frac{3M}{4\pi R^3} \frac{\xi_s}{3(-\theta'_s)} \theta^n \tag{11}$$

$$P = \frac{GM^2}{R^4} \frac{1}{4\pi(n+1)(\theta'_s)^2} \theta^{n+1} \tag{12}$$

$$T = \mu \frac{GM}{\mathscr{R}R} \frac{1}{(n+1)\xi_s(-\theta'_s)} \theta \tag{13}$$

$$\frac{M(r)}{M} = \left(\frac{\xi}{\xi_s}\right)^2 \frac{\theta'}{\theta'_s} \tag{14}$$

for $\xi \in [0, \xi_s]$. These are the quantities that, together with ε and L, are used in our study.

3. Numerical implementation

3.1. Solving the differential equation

The first step is defining and solving (4).

A fourth order Runge Kutta method is used, with initial conditions given by (5) and (6). Some points are of particular relevance and worth noting, namely:

1. The integration of the first step must be assured to work, avoiding the division by zero. This is done by analytically calculating the first step and using it as our starting point. This leads to new initial conditions in $\xi = \delta\xi$:
$$y_1(\delta\xi) \simeq 1 - \frac{(\delta\xi)^2}{2} \quad \text{and} \quad y_2(\delta\xi) \simeq -\delta\xi$$
2. It is important to accurately determine ξ_s, θ_s and $d\theta_s$, since these values are used in the structural equations found in section 2.3, so the maximum step of integration must be relatively small. It is also crucial to properly define the last step of integration. Assuming the star has no atmosphere, this is equivalent to taking only the solutions for $\theta \geq 0$, such that $\theta(\xi_s) = 0$. In order to optimize our algorithm, the numerical integration was set to finish when finding zero.

Fig. 1. Representation of the solution curves of the Lane-Emden equation for different values of n.

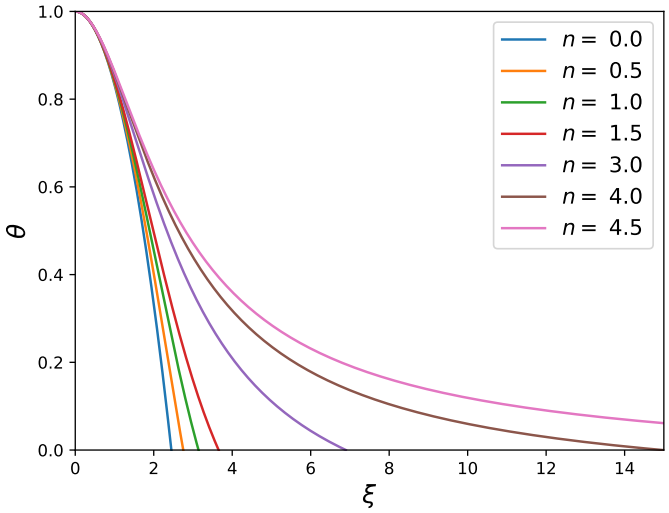

3.2. Estimating the luminosity

ρ, P, and T are obtained through the equations in section (2.3). Emissivity ε, as mentioned in the same section, is given by the nuclear reaction, and is quite straightforward to calculate. The next and, maybe, the most tricky step of this work, is determining the luminosity. In this process, it is important to bear in mind that:

1. Firstly, it is aimed to integrate equation (9). Once again, the final step of integration is a key element for the correctness of this step. To get L for each set of (ξ, θ, θ'), one must integrate until those points. So the integration is implemented with adaptative limits for each group of values.
2. To find the zeros of equation (10), one simply integrates for ξ corresponding to the star's surface, ξ_s, plugging in the radius R and mass M.

3.3. Code validation

The method is firstly validated through the verification of the solutions to the Lane-Emden equation for different values of n, which are presented in table (1).

Table 1. Solutions calculated for different values of n. They are according to what was expected, being a first validation of the algorithm provided.

n	ξ_s	$-\theta'_s$
0	2.4495	0.8164
1.0	3.1416	0.3183
1.5	3.6538	0.2033
3.0	6.8969	0.04242
4.0	14.9716	0.0080
4.5	31.8365	0.0017

The next validation method is a calculation of the emissivity $\varepsilon$for the Sun, for which data is very accurately known. The results are shown in figure (2), fitting once again what was expected (Monteiro (2019)): a peak around 17.5 erg/g/s for the PP chains, and a residual contribution due to the CNO cycle.

Fig. 2. Emissivity of the Sun. In blue, through PP chains, in orange due to the CNO cycle. Results are according to what was expected.

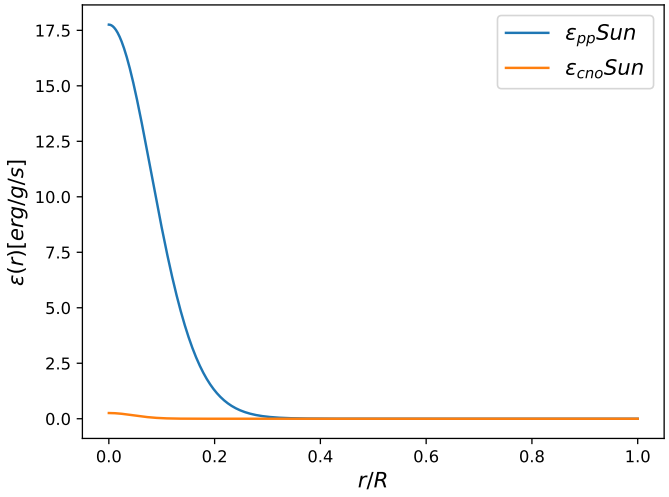

After estimating values of n, one may also calculate and use the potential energy of the polytrope, through equation (15) to obtain a new estimation of this value, and further validate our algorithm, as found in Monteiro (2019).

$$V \equiv -\int_0^M \frac{Gm}{r}\mathrm{d}m = -\frac{3}{5-n}\frac{GM^2}{R} \tag{15}$$

Using the set of solutions obtained from solving equation (4), this is equivalent to equation (16).

$$\frac{3}{5-n} = \frac{1}{\xi_s^3\theta_s'^2}\int_0^{\xi_s}\xi^3\theta^n(-\theta')\,\mathrm{d}\xi \tag{16}$$

Which may be used to test our numerical precision in the estimation ξ_s, θ_s and θ_s'. The difference between them is given by equation (17)

$$\Delta n = 3\xi_S^3\theta_S'^2\frac{1}{\int_0^{\xi_s}\xi^3\theta^n(-\theta')}\mathrm{d}\xi + 5 - n \tag{17}$$

Here n on the right being the value obtained originally.
The results of this verification are presented below in table 4.

4. Applications and results

The described method was implemented to three stars: Procyon A, Gliese 892 and γ Pavonis.

Table 2. Data for the stars used. Found on Boyajian et al. (2012) and Bruntt et al. (2010). Uniform chemical composition was assumed, and a mass fraction of helium of Y=0.27 was used.

Star	$R/R_\odot$	$M/M_\odot$	$L/L_\odot$	[FeH]
Gliese 892	0.778 ±0.005	0.81 ±0.03	0.265 ±0.002	0.07
Procyon A	2.13 ±0.06	1.46 ±.03	6.77 ±0.2	0.01
γPavonis	1.15 ±0.04	1.21 ±0.12	1.52 ±0.05	-0.74

Fig. 3. Density variation with the radius. One may see without much effort that most of the stars' masses are concentrated around their centers. Noting that Procyon A corresponds to the line in green and Gliese 892 the one in orange, it is also clear that, the heavier the star, the more centrally concentrated it is.

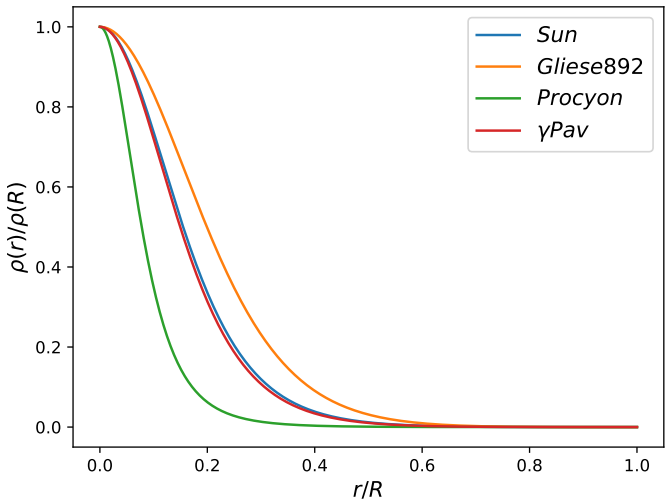

Fig. 4. Temperature variation with the radius. Following a similar line of thought, this plot shows that the lightest the star, the more homogeneous its temperature.

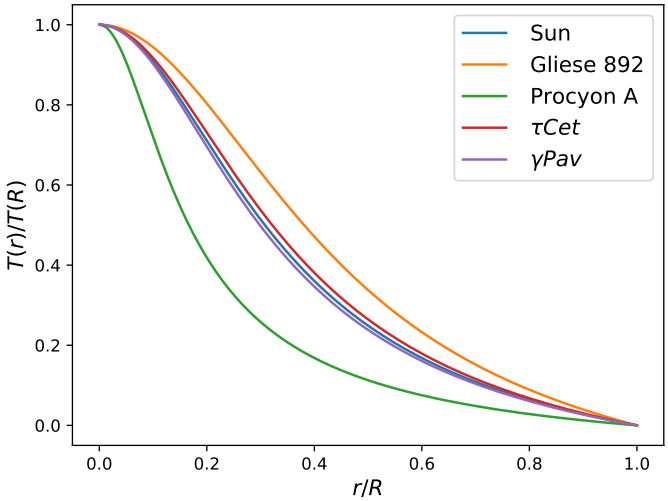

Implementing what has been described above for these stars and for the Sun, the graphs for $\rho(\xi)$, $P(\xi)$ and $T(\xi)$ were obtained and are presented in figures (3) to (5).

Here we can clearly see that, the more massive the star, the more concentrated these quantities are in the center.

For the emissivity, we can expect that, for sunlike stars, (mass in the range of $M/M_\odot \in [0.4, 1.5]$), we have an internal structure characterized by a radiative core surrounded by a convective envelope around their centers. In this case, the energy production is predominantly through PP chains.

In our study, for the stars γ Pavonis and Gliese 892, we found precisely that, as illustrated in figures 6 and 7. We were able to see that the emissivity through PP chains are, just like the case for the Sun, dominant. The CNO cycle starts to be more important for an increasing mass, the typical value considered for the importance of this process being $\sim 1.5M_\odot$ (Lang (2013)).

Fig. 5. Pressure variation with r. This plot resembles greatly the one for density, which is according to expected. The star's pressure increases towards the center, at a faster rate for more massive stars.

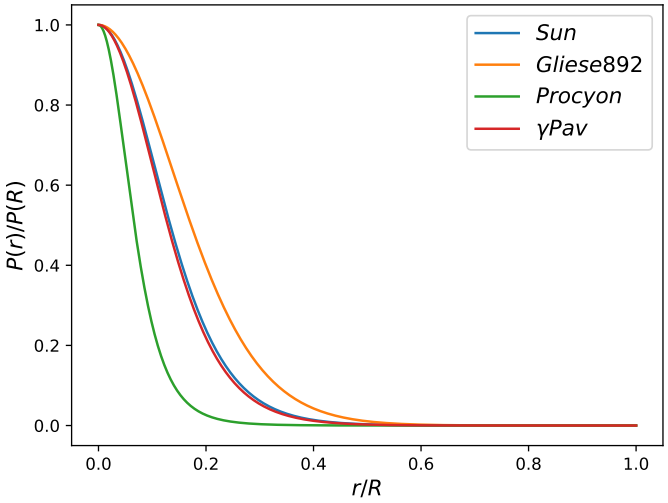

Fig. 6. Emissivity due to PP chains for the stars Gliese 892 and γ Pavonis. As expected, the emissivity is greater for the more luminous, larger star (data in table 2). This makes sense, since our method aims to find n such that the modeled emissivity allows an estimation of surface luminosity equal to the observed data.

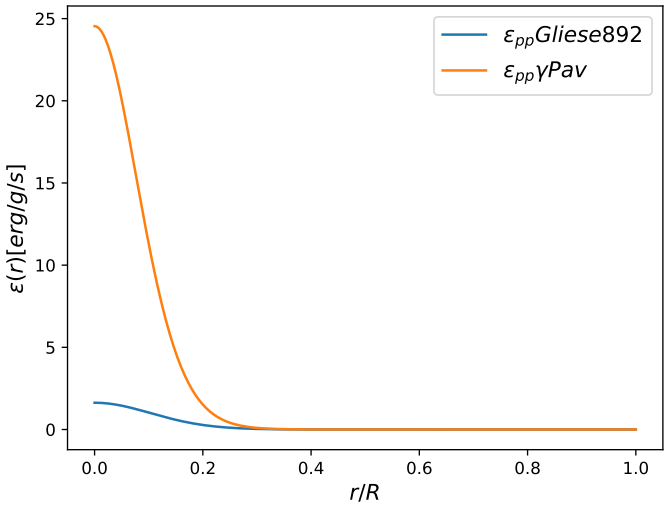

Fig. 7. Emissivity due to the CNO cycle for the stars Gliese 892 and γ Pavonis. Since these stars are very simillar to the Sun in terms of mass, radius and luminosity, it was expected a very small contribution to the energy production from the CNO cycle. This is precisely what was obtained.

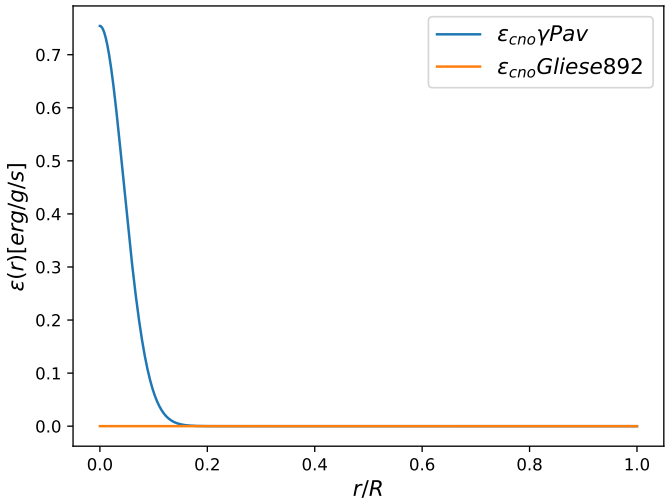

Fig. 8. Procyon's emissivity, according to our model. Note how the order of magnitude is significantly higher than the previous results.

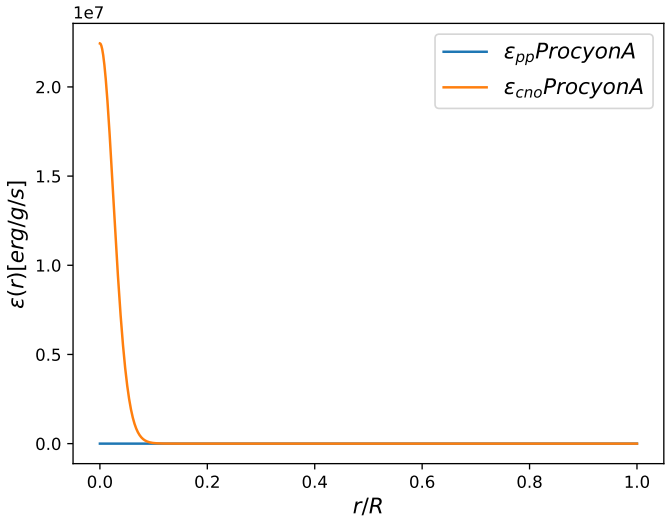

.pdf

4.1. Procyon A

For the star Procyon A, we have a somewhat different case, as one may see in figure 8. Since it is more massive, the core has higher temperatures, which allows the CNO cycle to dominate. This is a significantly more energetic process in comparison to PP chains (see equation 8) so it is expected that the emissivity is significantly higher, which was precisely what was verified. However, the order of magnitude found is notably larger than the previous obtained results (difference of 10^6), suggesting that this star is somewhat different than the other ones studied. Based on this relevant energetic difference, and considering this star's mass, radius and luminosity, one may wonder if this star belongs in the main sequence. Available research is not conclusive regarding the evolutionary stage of Procyon, but suggests that it is either at a late stage of the MS, or already evolving into a subgiant (Kervella et al. (2004)).

It is also relevant to note that, in comparison to the previous stars, this one has its emissivity more concentrated in its center, indicating a smaller, denser core.

Analyzing how luminosity varies with the distribution of mass, we also found a simillar behaviour to that of the other quantities studied.

4.2. Polytropic index determination and error estimation

Results for this value are presented in table 2.

Observing these results, one may immediately relate larger, more massive stars with values of n closer to 5.

The polytropic index found for the Sun was another suggestion that the algorithm provided works properly.

A repeated sample Monte-Carlo method was used to estimate the error on the determination of n, with a sample size of 1000. Basically, new values for R, M and L are generated in the range of their uncertainties using a normal distribution, and

Fig. 9. Luminosity vs mass distribution. The line for the Sun and for γ Pav coincide. The plot for Procyon is significantly more abrupt, indicating a more limited zone for the production of energy.

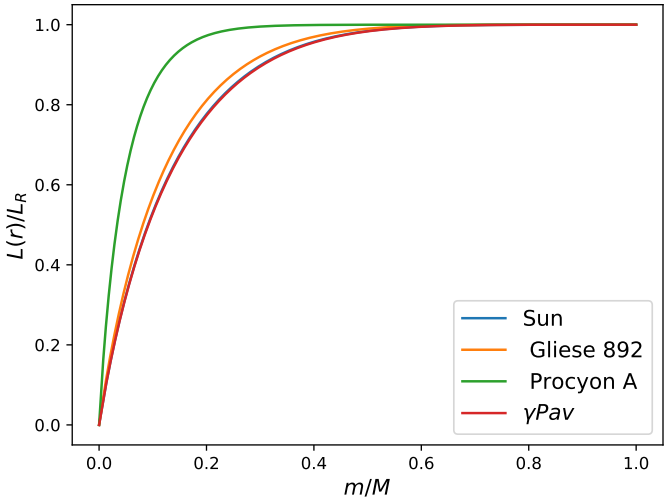

Table 3. Polytropic indices and their estimated errors for each star.

Star	n
Sun	3.1946 ±.0007
Gliese 892	2.71 ±0.07
Procyon A	4.04 ±0.03
γPavonis	3.2 ±0.1

a new n is calculated for each set of values. Their average and standard deviation σ_n are obtained, and the final result is given by $< n > \pm\sigma_n$.

A diagram showing a MC sampling for the star Gliese 892 is represented in figure 9.

Fig. 10. Monte Carlo method with 1000 samples for the error estimation for the star Gliese 892.

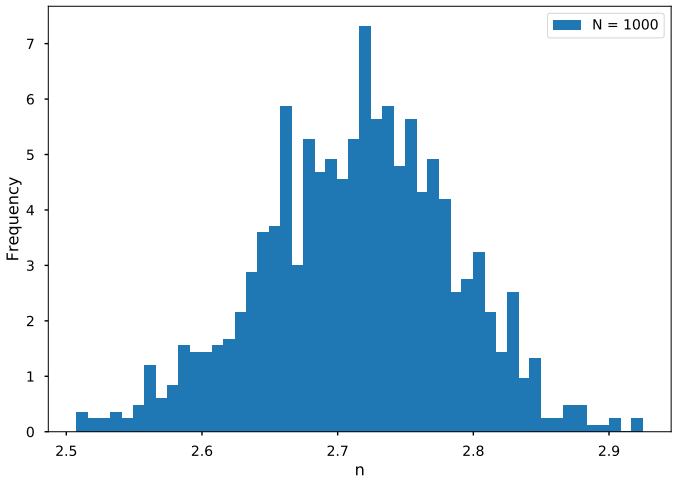

The calculation of Δn through equation (17) led us to the results in table 3. As one may see, the values obtained from the potential energy align nearly perfectly with the ones found initially, further validating a correct implementation of our method.

Table 4. Examples of the integration precision and result validation through equation (17).

Star	Δn
Sun	$1.62\text{x}10^{-10}$
Gliese 892	$1.95\text{x}10^{-10}$
γPavonis	$1.57\text{x}10^{-10}$

5. Results

5.1. Stellar structure

Our results suggest that the stars Gliese 892 and γ Pavonis are very simillar to the Sun in regards to structure, having a radiative core where PP chains are the main source of energy production, surrounded by a cooler, convective zone where energy is transported by the wheeling motion of convection.

Procyon A, of $\sim 1.46 M_\odot$, unlike the Sun is a star for which the main production of energy is the CNO cycle. It was noted, through plotting its emissivity, that the zone in which the cycle occurs is small and well defined (abrupt slope of the curve), suggesting the existence of a small and hot core. The predominance of the CNO cycle in such a confined region indicates that this star may have a different structure than the former two, since these hydrogen-burning reactions can cause the development of a convective core, which may then be overlaid by a radiation zone. (Provost et al. (2006))

On a more general note, we can infer from figures (3) to (5) that smaller, low-mass stars tend towards a more uniform composition, based on the smooth slope of the plotted curves. On the other hand, larger, high-mass stars, have better defined layers and denser, hotter cores.

As for the polytropic index, we can relate, for sunlike stars, larger values of n with with heavier, larger stars with a smaller, denser core where a more concentrated production of energy occurs. They have, thus, a higher effective temperature and luminosity. Through an attentive look at figures (6) and (7), one can conclude that greater values of n also mean a higher rate of consumption of hydrogen through the CNO cycle. This makes sense, since this process deals with heavy elements such as Carbon, Nitrogen and Oxygen (as the name suggests) that require higher conditions of temperature.

Our results also indicate that sunlike stars belong in a limited range of n, around 3, since for the star Procyon A, with an n of 4.04, a different behaviour was obtained.

5.2. Method and limitations

For the polytropic model to show meaningful results, an adequate estimation of the chemical composition of the star is necessary, as well as setting proper energy production equations, and having correct values for the mass, radius and luminosity. The model used in this work in particular aims to study main sequence, sunlike stars. So, for the study of other types of stars it isn't ideal as it won't reflect the star's true structure.

We're studying Procyon A as a MS star however, even if it would be classified as an early subgiant, burning hydrogen would still be its method of energy production. The only adjustment would then be the Helium fraction. The values of Helium fraction used in research regarding this star range $Y \in [0.26, 0.33]$ (Kervella et al. (2004)), which includes the value

used in this work (Y=0.27), so we may conclude that our model is reasonable for this case.

As mentioned in section 1, we simplify the initial problem to a large degree, further limiting the amount of systems we can study. The main simplification is the assumption that we can fully describe the star with a single polytropic index, since it ignores the existence of an atmosphere.

6. Conclusion

- The polytropic model for stellar interiors was studied in the case of main sequence stars. A process for the numerical implementation of this model was developed. This included setting adequate initial conditions for solving the Lane-Emden equation, integrating the obtained parameters so as to estimate a value for the polytropic index and validating our code.
- Our algorithm was implemented for the stars $\gamma Pavonis$ (slightly more massive than the Sun), Procyon A (significantly more massive and luminous than the Sun) and Gliese 892 (smaller than the Sun).
- We concluded that γ Pavonis and Gliese 892 are sunlike stars, having a simillar structure to the Sun: a radiative core surrounded by a convective envelope; and that Procyon A has small, hot convective core surrounded by a radiative layer.
- Their internal structures were further discussed, and general conclusions were drawn for stars that have different values of polytropic indix.
- Limitations to our model and improvements were analyzed.

References

Boyajian, T. S., von Braun, K., van Belle, G., et al. 2012, The Astrophysical Journal, 757, 112, arXiv: 1208.2431

Bruntt, H., Bedding, T. R., Quirion, P.-O., et al. 2010, Monthly Notices of the Royal Astronomical Society, 405, 1907

Kervella, P., Thévenin, F., Morel, P., et al. 2004, Astronomy & Astrophysics, 413, 251

Lang, K. R. 2013, The Life and Death of Stars (Cambridge University Press), google-Books-ID: NFYgAwAAQBAJ

Monteiro, Jorge Filipe S. Gameiro, & João José F. G. A. Lima. 2019, Astrofísica Estelar

Monteiro, M. J. P. 2019, Astronomia Computacional

Provost, J., Berthomieu, G., Martić, M., & Morel, P. 2006, Astronomy & Astrophysics, 460, 759